Correlation effects in MgO and CaO: Cohesive energies and lattice constants

Klaus Doll, Michael Dolg

Max-Planck-Institut für Physik komplexer Systeme
D-01187 Dresden, Germany

Hermann Stoll

Institut für Theoretische Chemie
Universität Stuttgart
D-70550 Stuttgart, Germany

January 12, 2014

Abstract

A recently proposed computational scheme based on local increments has been applied to the calculation of correlation contributions to the cohesive energy of the CaO crystal. Using *ab-initio* quantum chemical methods for evaluating individual increments, we obtain $\sim 80\%$ of the difference between the experimental and Hartree-Fock cohesive energies. Lattice constants corrected for correlation effects deviate by less than 1% from experimental values, in the case of MgO and CaO.

accepted by Phys. Rev. B

1 Introduction

Ab-initio Hartree-Fock (HF) and configuration interaction (CI) methods are standard tools in computational chemistry nowadays and various program packages are available for accurate calculations of properties of atoms and molecules. For solids, HF calculations have become possible, on a broad scale, with the advent of the program package CRYSTAL [1]. However, the problem of an accurate treatment of electron correlation is not fully settled (for a survey see [2]).

Although the absolute value of the HF energy is usually much larger than the correlation energy, the correlation energy is very important for energy differences. For example, the O^- ion is not stable at the HF level, and correlations are necessary in order to obtain even qualitative agreement with the experimental result for the electron affinity of oxygen. In solid state physics, NiO is a well known example of a system which is insulating due to correlations.

The most widely used method to include correlations in solids is density functional theory (DFT) [3]. DFT has also recently become quite popular for a computationally efficient treatment of exchange and correlation in molecules. However, a systematic improvement towards the exact results is currently not possible with DFT. Wave-function-based methods are more suitable for this purpose.

In the last years, Quantum Monte-Carlo calculations have been performed for several systems [4]. Correlations are included here by multiplying the HF wavefunction with a Jastrow factor. An approach more closely related to quantum chemistry is the Local Ansatz [5, 2] where judiciously chosen local excitation operators are applied to HF wavefunctions from CRYSTAL calculations. Some years ago, an incremental scheme has been proposed and applied in calculations for semiconductors [6, 7], for graphite [8] and for the valence band of diamond [9]; here information on the effect of local excitations on solid-state properties is drawn from calculations using standard quantum chemical program packages. In a recent paper [10] we showed that this method can be successfully extended to ionic solids; we reported results for the correlation contribution to the cohesive energy of MgO. In the present article, we apply the scheme to the cohesive energy of CaO, as a second example. In addition, we show how correlations affect the lattice constants of MgO and CaO. For these systems, several calculations have been performed at the HF level with the CRYSTAL code [11, 12, 13, 14, 15, 16] as well as with inclusion of correlations using DFT [12, 14, 15, 17].

2 The Method

The method of increments can be used to build up correlation effects in solids from local correlation contributions which in term may be obtained by transferring results from suitably embedded finite clusters to the infinite crystal. It has been fully described in [6, 7, 8, 10], and a formal derivation has been given within the framework of the projection technique [18]. Thus, we will only briefly repeat the main ideas.
(a) Starting from self-consistent field (SCF) calculations localized orbitals are generated which are assumed to be similar in the clusters and in the solid.
(b) One-body correlation-energy increments are calculated: in our specific case these are the correlation energies $\epsilon(A)$, $\epsilon(B)$, $\epsilon(C)$, ... of localized orbital groups which can be attributed to X^{2+} (X = Mg, Ca) or O^{2-} ions at ionic positions A, B, C, ... Each localized orbital group is correlated separately.
(c) Two-body increments are defined as non-additivity corrections:

$$\Delta\epsilon(AB) = \epsilon(AB) - \epsilon(A) - \epsilon(B),$$

where $\epsilon(AB)$ is the correlation energy of the joint orbital system of AB.
(d) Three-body increments are defined as

$$\begin{aligned}\Delta\epsilon(ABC) = \quad & \epsilon(ABC) - [\epsilon(A) + \epsilon(B) + \epsilon(C)] - \\ & [\Delta\epsilon(AB) + \Delta\epsilon(AC) + \Delta\epsilon(BC)].\end{aligned}$$

Similar definitions apply to higher-body increments.
(e) The correlation energy of the solid can now be expressed as the sum of all possible increments:

$$\epsilon_{\text{bulk}} = \sum_A \epsilon(A) + \frac{1}{2}\sum_{A,B} \Delta\epsilon(AB) + \frac{1}{3!}\sum_{A,B,C} \Delta\epsilon(ABC) + ... \qquad (1)$$

Of course, this only makes sense if the incremental expansion is well convergent, i.e. if $\Delta\epsilon(AB)$ rapidly decreases with increasing distance of the ions at position A and B and if the three-body terms are significantly smaller than the two-body ones. A pre-requisite is that the correlation method used for evaluating the increments must be size-extensive: otherwise the two-body increment $\Delta\epsilon(AB)$ for two ions A and B at infinite distance would not vanish. In our present work, we used three different size-extensive approaches, cf. Sect. 2.1. Finally, the increments must be transferable, i.e. they should only weakly depend on the cluster chosen.

2.1 Correlation Methods

In this section we want to give a brief description of the correlation methods used. In the averaged coupled-pair functional (ACPF [19]) scheme, the correlation energy is expressed in the form

$$E_{\rm corr}[\Psi_c] = \frac{<\Psi_{SCF}+\Psi_c|H-E_{SCF}|\Psi_{SCF}+\Psi_c>}{1+g_c<\Psi_c|\Psi_c>} \tag{2}$$

with Ψ_{SCF} being the SCF-wavefunction (usually of the spin-restricted Hartree-Fock type) and Ψ_c the correlation part of the wavefunction,

$$|\Psi_c>=\sum_{\substack{a\\r}} c_a^r a_r^+ a_a|\Psi_{SCF}> + \sum_{\substack{a<b\\r<s}} c_{ab}^{rs} a_r^+ a_s^+ a_a a_b|\Psi_{SCF}>; \tag{3}$$

g_c is chosen as $\frac{2}{n}$ in order to make the expression (2) approximately size-consistent (n being the number of correlated electrons). For more details (and the extension to multi-reference cases), see [19].
In the coupled-cluster singles and doubles (CCSD [20]) scheme, the wavefunction is expressed with the help of an exponential ansatz:

$$|\Psi_{CCSD}>=\exp(\sum_{\substack{a\\r}} c_a^r a_r^+ a_a + \sum_{\substack{a<b\\r<s}} c_{ab}^{rs} a_r^+ a_s^+ a_a a_b)|\Psi_{SCF}> . \tag{4}$$

a^+ (a) are creation (annihilation) operators of electrons in orbitals which are occupied (a, b) or unoccupied (r, s) in the SCF wavefunction.
Finally, in the CCSD(T) scheme, three particle excitations are included by means of perturbation theory as proposed in [21].
We used these three methods to compare their quality in applications to solids. It turns out that ACPF and CCSD give very similar results, while CCSD(T) yields slighty improved energies [22]. Altogether, the results are not strongly dependent on the methods and no problem arises, therefore, if only one method should be applicable (as is the case for low-spin open-shell systems, where CCSD and CCSD(T) are not yet readily available). All calculations of this work were done by using the program package MOLPRO [23, 24].

3 Cohesive Energy of CaO

3.1 Basis sets and test calculations

For calculating the correlation contribution to the cohesive energy of CaO, we closely follow the approach of Ref. [10]. For oxygen we choose a $[5s4p3d2f]$ basis set [25]. Calcium is described by a small-core pseudopotential replacing the $1s$, $2s$ and $2p$ electrons [26], and a corresponding $[6s6p5d2f1g]$ valence basis set (from ref. [26], augmented with polarization functions f_1=0.863492, f_2=2.142 and g=1.66) is used. All orbitals are correlated, with the exception of the O $1s$ core. In particular, the correlation contribution of the outer-core Ca $3s$ and $3p$ orbitals is explicitly taken into account. We did not use a large-core (X^{2+}) pseudopotential and a core polarization potential (CPP) for treating core-valence correlation as was done in the case of MgO [10], because Ca is close to the transition metals and excitations into d-orbitals are important. The influence of the latter on the X^{2+} core cannot be well represented by a CPP since the $3d$ orbitals are core-like themselves (cf. the discussion in [27]). Correlating the Ca outer-core orbitals explicitly, using the small-core (Ca^{10+}) pseudopotential, we circumvent this problem.

Using this approach, we performed test calculations for the first and second ionization potential of the Ca atom (Table 1) and calculated spectroscopic properties of the CaO molecule (Table 2). In both cases, we obtain good agreement with experiment.

3.2 Intra-atomic Correlation

We first calculated one-body correlation-energy increments. For Ca^{2+}, the results are virtually independent of the solid-state surroundings. This was tested by doing calculations for a free Ca^{2+} and a Ca^{2+} embedded in point charges. (A cube of 7x7x7 ions was simulated by point charges ± 2, with charges at the surface planes/edges/corners reduced by factors 2/4/8, respectively.)

In the case of O^{2-}, of course, the solid-state influence is decisive for stability, and we took it into account by using an embedding similar to that of Ref. [10]: the Pauli repulsion of the 6 nearest Ca^{2+} neighbours was simulated by large-core pseudopotentials [28], while the rest of a cube of 7x7x7 lattice sites was treated in point-charge approximation again. A NaCl-like structure with a lattice constant of 4.81 Å was adopted. (The experimental value for the lattice constant is 4.8032 Å at a temperature of T=17.9 K [29]). We performed similar calculations for various other finite-cluster approximations of the CaO crystal, in order to insure that the results

are not sensitive to lattice extensions beyond the cube mentioned above.

The results for the one-body correlation-energy increments are shown in Table 3. It is interesting to note that the absolute value of the Ca $\rightarrow$ Ca^{2+} increment is larger than in the case of Mg, although the electron density in the valence region of Ca is lower than for Mg. The larger correlation contribution for Ca can be rationalized by the fact that excitations into low-lying unoccupied *d*-orbitals are much more important for Ca than for Mg. This is a result which would be difficult to explain by density functional theory: in a local-density framework, higher density leads to a higher absolute value of the correlation energy.

In Ref. [10] we argued that the increment in correlation energy ϵ(embedded O^{2-}) $-\epsilon$(free O) is not just twice the increment ϵ(free O^{-}) $-\epsilon$(free O). However, comparing the increments ϵ (embedded O^{2-}) $-\epsilon$(embedded O) and ϵ (embedded O^{-}) $-\epsilon$(embedded O) one finds a factor very close to two. This can be seen from Table 4 where we compare the increments in the case of MgO. Thus, for the embedded species linear scaling is appropriate as in the case of the gas-phase isoelectronic series Ne, Ne^{+}, Ne^{2+}: there, the increments in correlation energy are 0.0608 H (Ne^{2+} $\rightarrow$ Ne^{+}) and 0.0652 H (Ne^{+} $\rightarrow$ Ne) [30]. Table 4 also shows that the correlation contribution to the electron affinity of the oxygen atom is *smaller* for the embedded species than in the gas phase. This is due to the fact that energy differences to excited-state configurations become larger when enclosing O^{n-} in a solid-state cage. Once again, this is at variance with a LDA description as the electron density in the case of the embedded O^{-} is more compressed than in the case of a free O^{-}.

In Figure 1 we show the charge density distribution of O^{2-}, again in the case of MgO. We used basis functions on both O and Mg; the Mg $1s$, $2s$ and $2p$-electrons are replaced by a pseudopotential. One recognizes the minimum near the Mg^{2+} cores, where the Pauli repulsion prevents the oxygen electrons from penetrating into the Mg^{2+} core region. This way, the solid is stabilized. The 6^{th} contour line, counting from Mg to O, is the line which represents a density of 0.002 a.u. This is the density which encloses about 95 % of the charge and was proposed as an estimate of the size of atoms and molecules [31].

The sum of the intra-ionic correlation-energy increments discussed in this subsection turns out to yield only $\sim$ 60 % of the correlation contribution of the cohesive energy of CaO. This percentage is quite similar to that obtained for MgO [10], at the same level. Thus, although MgO and CaO are to a very good approximation purely ionic solids, the inter-atomic correlation effects

to be dealt with in the next subsection play an important role.

3.3 Two- and three-body increments

When calculating two-body correlation-energy increments, point charges or pseudopotentials surrounding a given ion have to be replaced by 'real' ions. In the case of an additional 'real' O^{2-}, its next-neighbour shell also has to be replaced by a cage of pseudopotentials simulating Ca^{2+}. This way the increments shown in Table 3 are obtained.

It turns out that the Ca-O increments are much more important than the O-O increments, while Ca-Ca increments are negligibly small. The changes with respect to MgO [10] can easily be rationalized: On the one hand, the lattice constant is larger than in the case of MgO (4.81 Å vs. 4.21 Å), which reduces the van der Waals interaction and makes the O-O increments smaller. On the other hand, the polarizability of Ca^{2+} is by a factor of more than 6 higher than that of Mg^{2+} (see for example Ref. [28]), which leads to large Ca-O increments. We show the van der Waals-like decay in Figure 2 by plotting the two-body increments O-O for CaO from CCSD calculations (without including weight factors). By multiplying with the sixth power of the distance, one can verify the van der Waals-law. Plots for the other two-body increments are qualitatively similar.

Three-body increments contribute with less than 2 % to the correlation piece of the bulk cohesive energy and may safely be neglected, therefore. A survey of the convergency pattern of the incremental expansion, for both CaO and MgO, is given in Figs. 3 and 4.

3.4 Sum of increments

Adding up the increments of sections 3.2 and 3.3 (cf. Table 5), we obtain between 71 and 78 % of the 'experimental' correlation contribution to the cohesive energy which we define as the difference of the experimental cohesive energy (11.0 eV, [32]) plus the zero-point energy (which is taken into account within the Debye approximation and is of the order 0.1 eV) minus the HF binding energy (7.6 eV, Ref. [13]). The percentage obtained is slightly less compared to the case of MgO [10] where 79 to 86 % were recovered. One of the reasons for this difference is that we used a CPP in the case of MgO which covers nearly 100% of the core-valence correlation contributions in Mg, while the explicit treatment of that correlation piece for Ca was less exhaustive. Another reason is that on the Hartree-Fock level f-functions for

Ca (which are not yet implemented in CRYSTAL) would probably increase the cohesive energy and lower the 'experimental' correlation contribution. Finally, as in the case of MgO, a significant part of the missing correlation energy should be due to basis set errors for the O atom. – The total cohesive energy recovered in our calculations is in the range of between 91 and 93 % of the experimental value.

Our results are compared in Table 5 to those from density functional calculations. We choose the results from [12] where a correlation-only functional was used and 0.078 to 0.097 H of the correlation contribution to the cohesive energy were obtained, depending on the specific correlation functional used.

4 Lattice constants

At the Hartree-Fock level, the lattice constant is in good agreement with experiment for MgO [11, 12, 14, 15, 16], whereas there is a deviation of 0.05 Å in the case of CaO [13]. It is interesting, therefore, to study the influence of correlation effects on lattice constants. In Tables 6 and 7, we give the necessary increments for MgO and CaO, respectively. We find two main effects of correlations. On the one hand, the van der Waals-interaction leads to a reduction of the lattice spacing since the attractive interaction is of the form $-\frac{1}{r^6}$ and obviously stronger at shorter distance. On the other hand, we find that the intra-ionic correlation of the O^{2-}-ion forces a larger constant. This can be understood from the argument that excited configurations are lower in energy and mix more strongly with the ground-state determinant if the O^{2-} is less compressed as explained in section 3.2.

Adding up all these contributions (cf. Table 8), they are found to nearly cancel in the case of MgO and to lead to a reduction of only 0.01 Å . For obtaining this result, we applied a linear fit to the correlation energy and superimposed it on the HF potential curve of Refs. [16, 13]. We checked the validity of the linear approximation by calculating selected increments at other lattice constants.

In the case of CaO, the van der Waals-interaction is more important and the lattice constant is reduced to 4.81 Å which is in nice agreement with the experimental value. The lattice constants seem to be in better agreement with the experimental values than those calculated from density functional theory for MgO [14, 15] and CaO [14], where deviations of ± 2 % are found. This is similar to earlier findings for semiconductors [7].

5 Conclusion

We determined the correlation contribution to the cohesive energy of CaO using an expansion into local increments recently applied to MgO. Making use of quantum-chemical *ab-initio* configuration-interaction calculations for evaluating individual increments, we obtain ~ 80 % of the expected value. The missing energy is probably mainly due to the lack of g and higher polarization functions in our one-particle basis set. The computed lattice constants show deviations of less than 1% from the experimental values. We found two correlation effects on the lattice constants: the inter-atomic van der Waals-force leads to a reduction, whereas intra-atomic correlations of the O^{2-} ions lead to an increase of the lattice constant.

The main difference between CaO and MgO is the reduced importance of the inter-atomic O-O correlations in CaO (due to the larger lattice constant) and the higher importance of the Ca-O correlations (due to the higher polarizability of Ca^{2+}).

Compared to DFT, the numerical effort of our scheme is significantly higher. However, we feel that the advantage of the present approach is the high quality and stability of the results both for atoms, ions as well as for solids. Another advantage is the possibility of a systematic improvement by using larger basis sets.

We think that the method of local increments is capable now of being routinely applied to ionic systems, and a systematic study on alkali halides is underway. An extension to open-shell systems such as NiO is also a project currently under investigation.

Acknowledgments

We would like to thank Prof. P. Fulde for supporting this work and Prof. W. C. Nieuwpoort (Groningen) for interesting suggestions. We are grateful to Prof. H.-J. Werner (Stuttgart) for providing the program package MOLPRO.

References

[1] R. Dovesi, C. Pisani, and C. Roetti, Int. J. Quantum Chem. **17**, 517 (1980); C. Pisani, R. Dovesi, and C. Roetti, Lecture Notes in Chemistry, vol. 48 (Springer, Berlin, 1988)

[2] P. Fulde in *Electron Correlations in Molecules and Solids*, Springer Series in Solid State Sciences, vol. 100 (Springer, Berlin, 1993)

[3] For a review about DFT, see, e.g. R. O. Jones, O. Gunnarsson, Rev. Mod. Phys. **61**, 689 (1989)

[4] S. Fahy, X. W. Wang, S. G. Louie, Phys. Rev. Lett. **61**, 1631 (1988); S. Fahy, X. W. Wang, S. G. Louie, Phys. Rev. B **42**, 3503 (1990); X.-P. Li, D. M. Ceperley, R. M. Martin, Phys. Rev. B **44**, 10929 (1991); L. Mitáš, R. M. Martin, Phys. Rev. Lett. **72**, 2438 (1994)

[5] G. Stollhoff, P. Fulde, J. Chem. Phys. **73**, 4548 (1980)

[6] H. Stoll, Phys. Rev. B **46**, 6700 (1992); H. Stoll, Chem. Phys. Lett. **191**, 548 (1992)

[7] B. Paulus, P. Fulde, H. Stoll, Phys. Rev. B **51**, 10572 (1995)

[8] H. Stoll, J. Chem. Phys. **97**, 8449 (1992)

[9] J. Gräfenstein, H. Stoll, P. Fulde, Chem. Phys. Lett. **215**, 611 (1993)

[10] K. Doll, M. Dolg, P. Fulde, H. Stoll, Phys. Rev. B **52**, 4842 (1995)

[11] M. Causà, R. Dovesi, C. Pisani, C. Roetti, Phys. Rev. B **33**, 1308 (1986)

[12] R. Dovesi, C. Roetti, C. Freyria-Fava, E. Aprà, V.R. Saunders, and N.M. Harrison, Philos. Trans. R. Soc. London Ser. A **341**, 203 (1992);

[13] W. C. Mackrodt, N. M. Harrison, V. R. Saunders, N. L. Allan, M. D. Towler, E. Aprà, R. Dovesi, Philos. Mag. A **68**, 653 (1993)

[14] M. Causà, A. Zupan, Chem. Phys. Lett. **220**, 145 (1994)

[15] M. I. McCarthy, N. M. Harrison, Phys. Rev. B **49**, 8574 (1994)

[16] M. Catti, G. Valerio, R. Dovesi, M. Causà, Phys. Rev. B **49**, 14179 (1994)

[17] N. C. Pyper, Phil. Trans. R. Soc. London A **352**, 89 (1995)

[18] T. Schork, Thesis, University Stuttgart (1992)

[19] R. J. Gdanitz, R. Ahlrichs, Chem. Phys. Lett. **143**, 413 (1988)

[20] F. Koester, H. Kümmel, Nucl. Phys. **17**, 477 (1960); J. Číček, J. Chem. Phys. **45**, 4256 (1966); J. Paldus, J. Číček, Phys. Rev. A **5**, 50 (1972); R. F. Bishop, Theor. Chim. Acta **80**, 95 (1991); G. D. Purvis III, R. J. Bartlett, J. Chem. Phys. **76**, 1910 (1982)

[21] K. Raghavachari, G. W. Trucks, J. A. Pople, M. Head-Gordon, Chem. Phys. Lett. **157**, 479 (1989)

[22] It was pointed out by H.-J. Werner that CCSD(T) as implemented in Ref. 23 can not be applied to localized orbitals but only to canonical ones (see M. J. O. Deegan, P. J. Knowles, Chem. Phys. Lett. **227**, 321 (1994)). In our scheme localization is necessary, but we can estimate the magnitude of the concomitant errors by calculating two-body increments using *different* clusters which makes localization unnecessary: a cluster with two oxygen atoms, e.g., in order to get $\epsilon(AB)$ and a cluster with one oxygen atom to get $\epsilon(A)$. We compared the increments $\Delta\epsilon(AB)$ calculated by using localized/canonical orbitals and found that the error for the most important increment is less than 0.01 eV including the weight factor. – The ACPF and CCSD results are not affected from this problem.

[23] MOLPRO is a package of *ab initio* programs written by H.-J. Werner and P.J. Knowles, with contributions from J. Almlöf, R.D. Amos, M.J.O. Deegan, S.T. Elbert, C. Hampel, W. Meyer, K. Peterson, R. Pitzer, A.J. Stone, and P.R. Taylor; the CPP program was written by A. Nicklass.

[24] H.-J. Werner and P.J. Knowles, J. Chem. Phys. **82**, 5053 (1985); P.J. Knowles and H.-J. Werner, Chem. Phys. Lett. **115**, 259 (1985); H.-J. Werner and P.J. Knowles, J. Chem. Phys. **89**, 5803 (1988); P.J. Knowles and H.-J. Werner, Chem. Phys. Lett. **145**, 514 (1988); H.-J. Werner and P.J. Knowles, Theor. Chim. Acta **78**, 175 (1990); C. Hampel, K. Peterson, and H.-J. Werner, Chem. Phys. Lett. **190**, 1 (1992); P.J. Knowles, C. Hampel, and H.-J. Werner, J. Chem. Phys. **99**, 5219 (1993)

[25] T.H. Dunning, Jr., J. Chem. Phys. **90**, 1007 (1989)

[26] M. Kaupp, P. v. R. Schleyer, H. Stoll, H. Preuss, J. Chem. Phys. **94**, 1360(1991)

[27] W. Müller, J. Flesch, and W. Meyer, J. Chem. Phys. **80**, 3297 (1984)

[28] P. Fuentealba, L. v. Szentpály, H. Preuss and H. Stoll, J. Phys. B **18**, 1287 (1985)

[29] K.-H. Hellwege and A. M. Hellwege (eds.), Landolt-Börnstein tables, Group III, Vol. 7b1 (Springer, Berlin, 1975)

[30] E.R. Davidson, S.A. Hagstrom, S.J. Chakravorty, V.M. Umar, and Ch. Froese-Fischer, Phys. Rev. A **44**, 7071 (1991)

[31] R. F. Bader, W. H. Henneker, P. E. Cade, J. Chem. Phys. **46**, 3341 (1967)

[32] CRC Handbook of Chemistry ad Physics, 75^{th} edition, Editor: David R. Lide (CRC Press, Boca Raton, 1994/1995)

[33] C. E. Moore, Atomic Energy Levels, NSRDS-NBS 35 / Vol. I-III, Nat. Bur. Standards (Washington, DC)

[34] K. P. Huber, G. Herzberg, Molecular Spectra and Molecular Structure: IV. Constants of Diatomic Molecules (Van Nostrand, New York, 1979)

[35] J. A. Irvin, P. J. Dagdigian, J. Chem. Phys. **73**, 176 (1980)

Table 1: Atomic ionization potentials $Ca \rightarrow Ca^{+}/Ca^{+} \rightarrow Ca^{2+}$ (in eV)

RHF	5.16/11.35
ACPF	6.01/11.78
CCSD	6.03/11.77
CCSD(T)	6.09/11.80
expt. [33]	6.11/11.87

Table 2: Bond length R_e (Å), dissociation energy D_e (eV) and vibrational frequency ω_e (cm^{-1}) of the CaO molecule.

	R_e	D_e	ω_e
RHF	1.812	0.67	829
CCSD	1.822	3.39	769
CCSD(T)	1.846	3.84	681
expt. [34, 35]	1.822	4.16±0.07	732.1

Table 3: Local increments (a.u.) for CaO at a lattice constant of 4.81 Å.

	weight[a]	ACPF	CCSD	CCSD(T)
$Ca \rightarrow Ca^{2+}$	1	+0.047045	+0.047359	+0.050921
$O \rightarrow O^{2-}$	1	-0.096104	-0.097083	-0.102340
sum of one-body increments		-0.049059	-0.049724	-0.051419
Ca – O next neighbour	6	-0.037704	-0.035436	-0.040266
Ca – O, 2^{nd} next neighbour	8	-0.000880	-0.000928	-0.001056
Ca – O, 3^{rd} next neighbour	24	-0.000288	-0.000504	-0.000576
Ca – O, 4^{th} next neighbour	30	-0.000150	-0.000090	-0.000120
Ca – Ca, next neighbour	6	-0.001002	-0.001026	-0.001128
Ca – Ca, 2^{nd} next neighbour	3	-0.000054	-0.000057	-0.000063
Ca – Ca, 3^{rd} next neighbour	12	-0.000060	-0.000072	-0.000072
O – O, next neighbour	6	-0.006888	-0.006402	-0.007548
O – O, 2^{nd} next neighbour	3	-0.000363	-0.000345	-0.000402
O – O, 3^{rd} next neighbour	12	-0.000324	-0.000312	-0.000360
O – O, 4^{th} next neighbour	6	-0.000066	-0.000066	-0.000078
O – O, 5^{th} next neighbour	12	-0.000060	-0.000060	-0.000078
O – O, 6^{th} next neighbour	4	-0.000016	-0.000008	-0.000016
sum of two-body-increments		-0.047855	-0.045306	-0.051763
O – O – O [b]	8	+0.000224	+0.000176	+0.000200
O – O – O [c]	12	+0.000060	+0.000036	+0.000048
O – Ca – Ca [d]	12	+0.000036	+0.000288	+0.000276
O – Ca – Ca [e]	3	-0.000078	-0.000015	-0.000030
O – Ca – O [f]	12	+0.000792	+0.001092	+0.000972
O – Ca – O [g]	3	-0.000180	-0.000060	-0.000132
O – Ca – O [h]	24	-0.000048	+0.000216	+0.000192
sum of three-body increments		+0.000692	+0.001685	+0.001412
total sum		-0.096342	-0.093445	-0.101910

[a] Weight factor in the incremental expansion of the bulk correlation energy (in a.u. per primitive unit cell) of CaO.

[b] ions at (1,0,0), (0,1,0) and (0,0,1)

[c] ions at (1,0,0), (-1,0,0) and (0,0,1)

[d] O at (0,0,0), Ca at (0,0,1) and (0,1,0)

[e] O at (0,0,0), Ca at (0,0,1) and (0,0,-1)

[f] O at (0,0,0) and (0,1,1), Ca at (0,1,0)

[g] O at (1,0,0) and (-1,0,0), Ca at (0,0,0)

[h] O at (0,0,0) and (0,1,1), Ca at (1,0,0)

Table 4: Intra-ionic correlation of free and embedded oxygen (in a.u.).

	incr. $O \rightarrow O^-$	incr. $O \rightarrow O^{2-}$
O and O^- free, O^{2-} embedded	0.062794	0.096460
O, O^-, O^{2-} embedded	0.050474	0.100715

Table 5: Correlation contributions to the cohesive energy of CaO (in a.u.).

ACPF	CCSD	CCSD(T)	DFT	expt.
0.095	0.092	0.101	0.078 ... 0.097 [12]	0.129

Table 6: Local increments (in a.u.) for MgO at a lattice constant of 4.18 Å

	ACPF	CCSD	CCSD(T)
$Mg \rightarrow Mg^{2+}$	+0.046897	+0.046897	+0.046897
$O \rightarrow O^{2-}$	-0.094833	-0.095808	-0.100867
one-body increments	-0.047936	-0.048911	-0.053970
Mg-O increments	-0.019750	-0.019798	-0.019804
O-O increments	-0.018516	-0.017229	-0.020154
two-body increments	-0.038266	-0.037027	-0.039958
three-body increments	+0.000847	+0.000818	+0.000862
sum at 4.18 Å	-0.085355	-0.085120	-0.093066
sum at 4.21 Å	-0.085233	-0.084909	-0.092983

Table 7: Local increments (in a.u.) for CaO at a lattice constant of 4.864 Å

	ACPF	CCSD	CCSD(T)
$Ca \rightarrow Ca^{2+}$	+0.047046	+0.047359	+0.050921
$O \rightarrow O^{2-}$	-0.097060	-0.098043	-0.103456
one-body increments	-0.050014	-0.050684	-0.052535
Ca-O increments	-0.037258	-0.035258	-0.040126
O-O increments	-0.007527	-0.006984	-0.008263
Ca-Ca increments	-0.001038	-0.001059	-0.001179
two-body increments	-0.045823	-0.043301	-0.049568
three-body increments	+0.000632	+0.001662	+0.001484
sum at 4.864 Å	-0.095205	-0.092323	-0.100619
sum at 4.81 Å	-0.096342	-0.093445	-0.101910

Table 8: Lattice constants of MgO and CaO (in Å).

System	RHF	ACPF	CCSD	CCSD(T)	DFT	exp.
MgO	4.191 [16]	4.181	4.173	4.184	4.11 ... 4.27 [14] 4.101 ... 4.105 [15]	4.2072 [29]
CaO	4.864 [13]	4.809	4.805	4.801	4.73 ... 4.85 [14]	4.8032 [29]

Figure 1: Charge density of embedded O^{2-}

Figure 2: Van der Waals-like decay of the two-body O-O increments in CaO

Figure 3: Sum of local increments for MgO

Figure 4: Sum of local increments for CaO

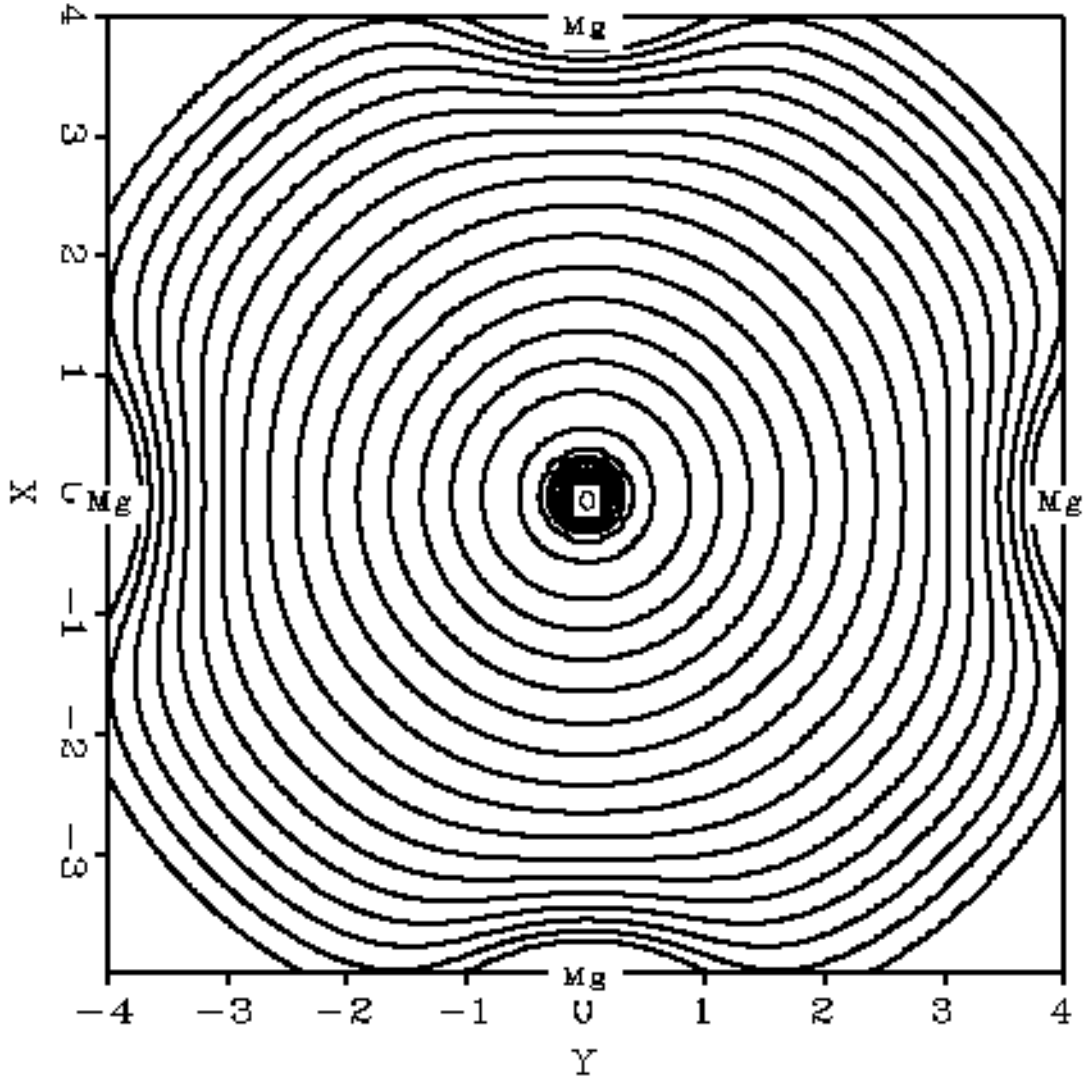

CHARGE DENSITY

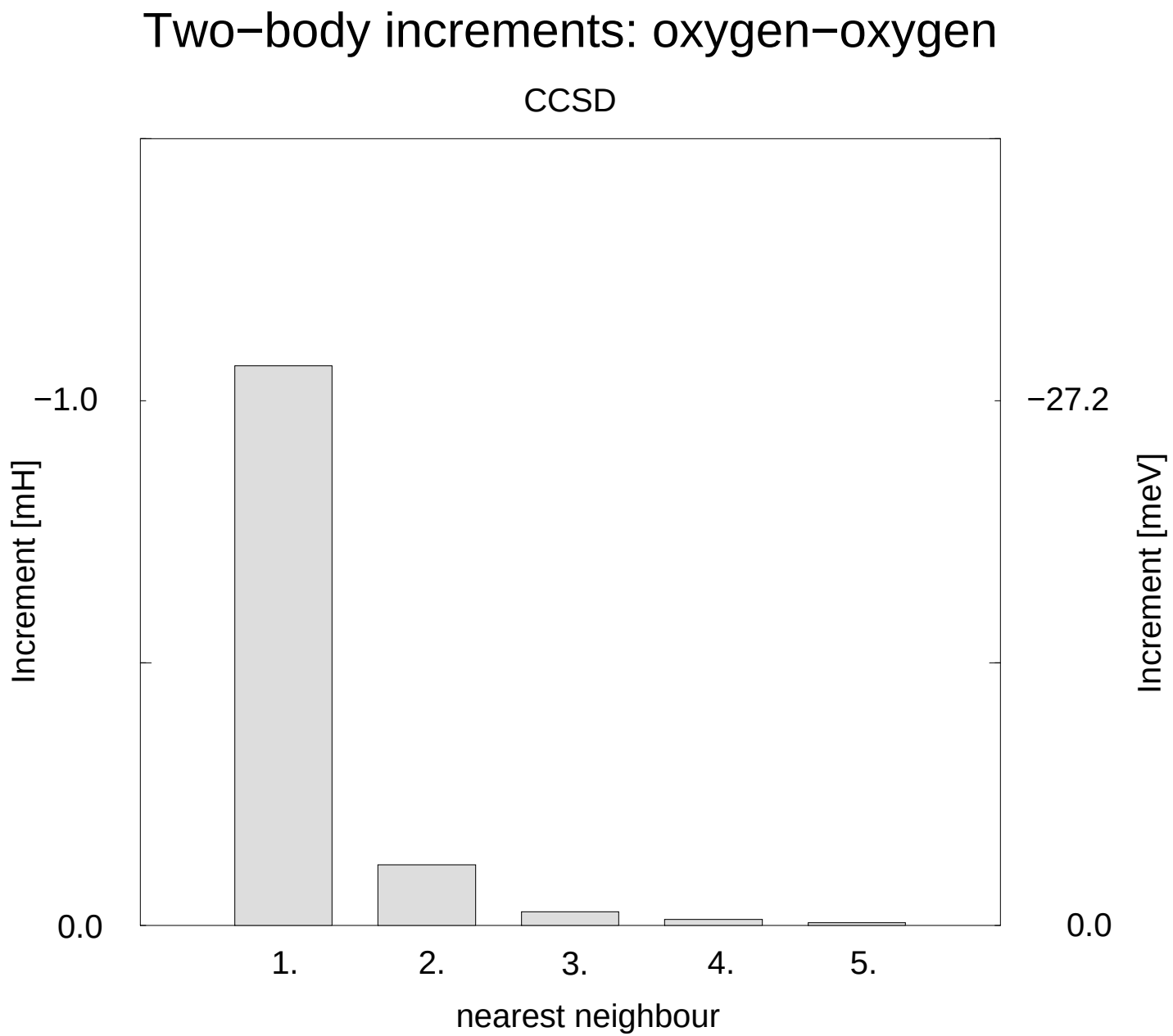
Two−body increments: oxygen−oxygen
CCSD
−1.0
0.0
Increment [mH]
−27.2
0.0
Increment [meV]
1.
2.
3.
4.
5.
nearest neighbour

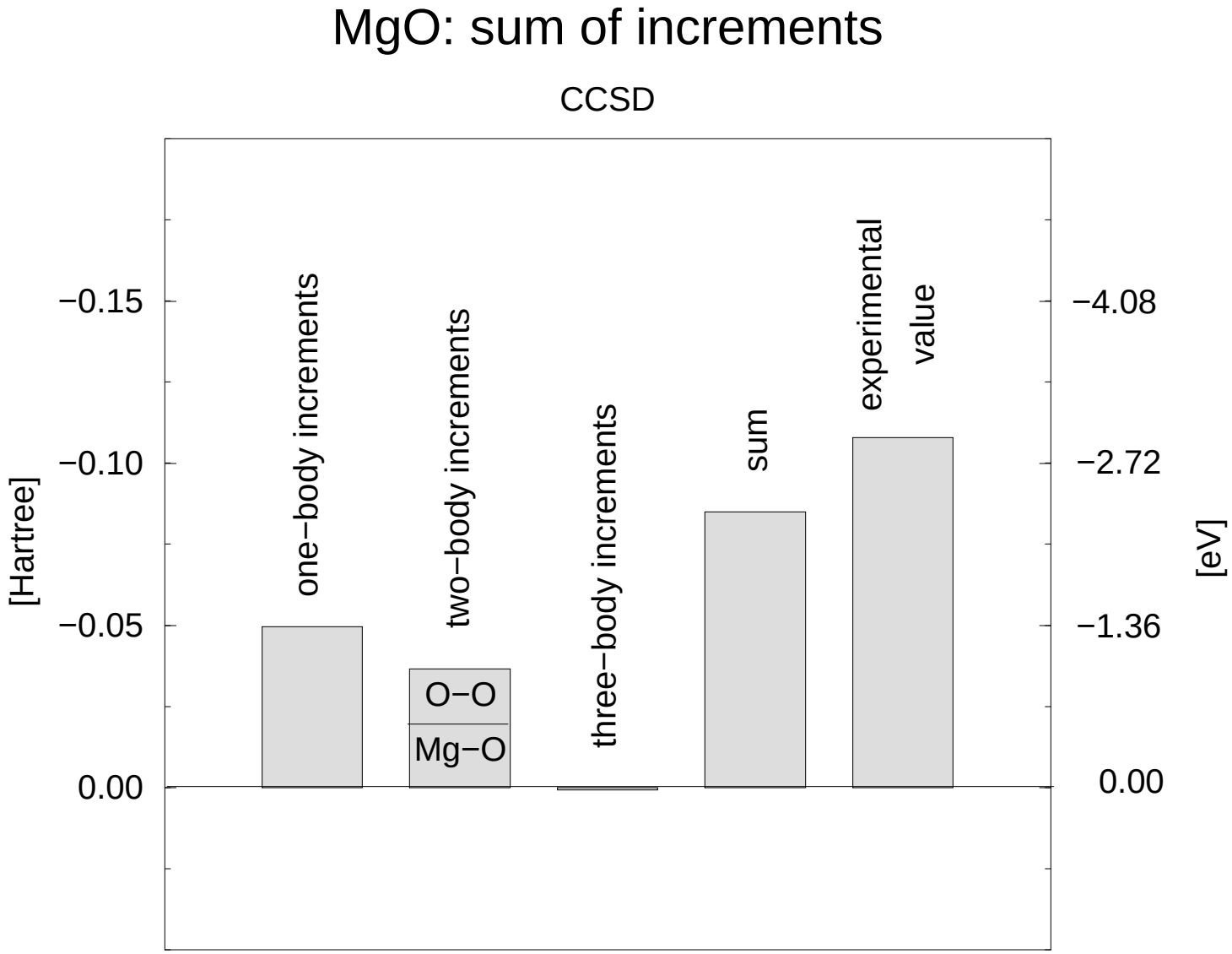
MgO: sum of increments
CCSD
[Hartree]
−0.15
−0.10
−0.05
0.00
one−body increments
two−body increments
O−O
Mg−O
three−body increments
sum
experimental value
−4.08
−2.72
−1.36
0.00
[eV]

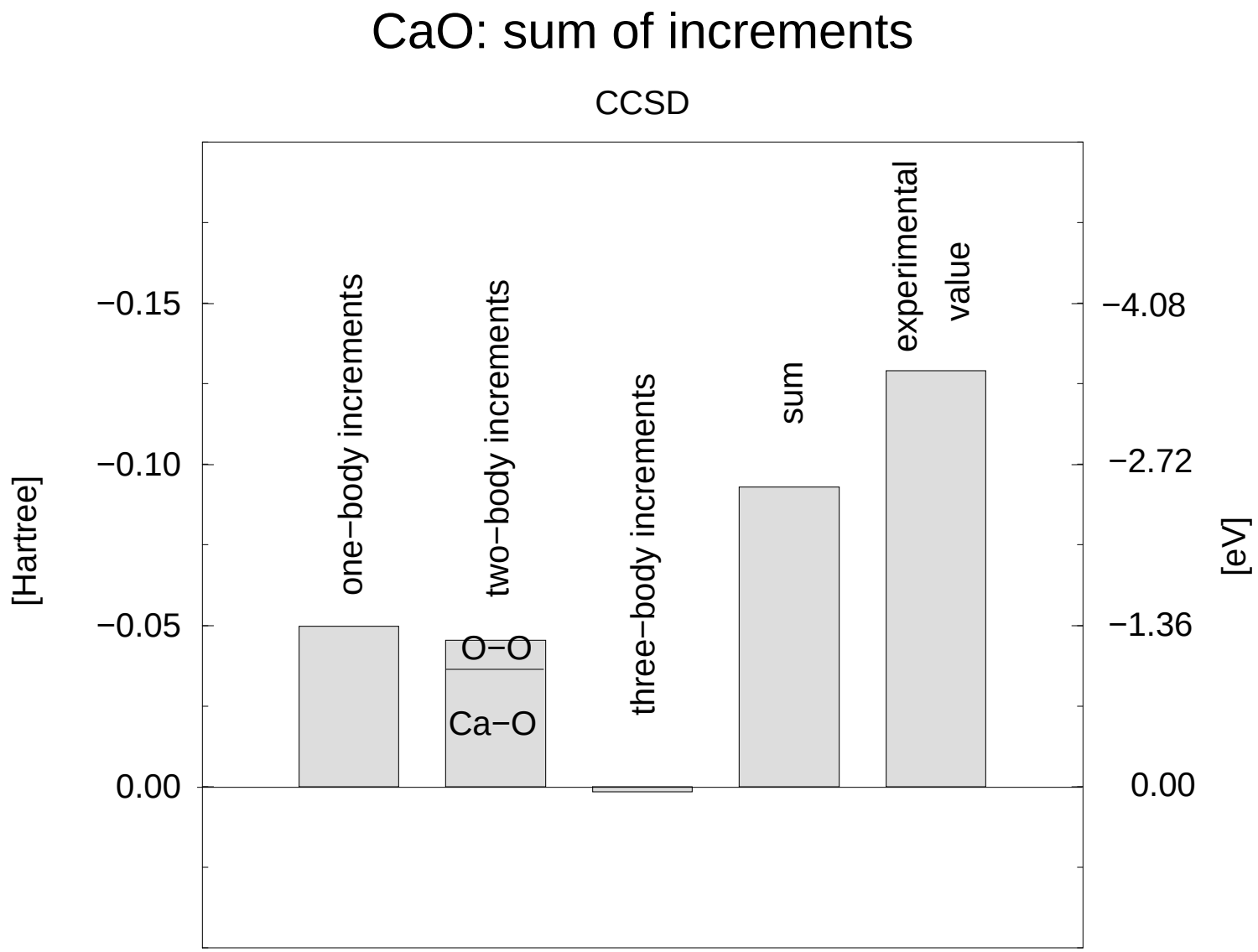
CaO: sum of increments
CCSD
[Hartree]
−0.15
−0.10
−0.05
0.00
one−body increments
two−body increments
O−O
Ca−O
three−body increments
sum
experimental
value
−4.08
−2.72
−1.36
0.00
[eV]